

# Thermochemical Valorization of Açai (Euterpe oleracea) Seeds: a Study using Gibbs Energy Minimization and Entropy Maximization Methods

Yan Caio Morais da Costa<sup>a</sup>, Ana Carolina Portela Pessoa Coelho<sup>a</sup>, Julles Mitoura dos Santos Júnior<sup>b</sup>, Annamaria Dória Souza Vidotti<sup>a</sup>, Antonio Carlos Daltro de Freitas<sup>b</sup>, Reginaldo Guirardello<sup>a\*</sup>

<sup>a</sup>Federal University of Maranhão: Chemical Engineering Department, São Luís - MA, Brazil

<sup>b</sup>School of Chemical Engineering, University of Campinas (UNICAMP), Campinas - SP, Brazil  
[guira@feq.unicamp.br](mailto:guira@feq.unicamp.br)

The use of biomass as a primary source for production of hydrogen (H<sub>2</sub>) and synthesis gas (syngas) has gained significant attention due to its potential to diversify the global energy matrix. An example of biomass particularly relevant to Brazil is *Euterpe oleracea*, commonly known as açai. The seeds of this fruit account for approximately 70% of its mass and are a major by-product of açai pulp production. In this work, the thermodynamic analysis was performed using Gibbs energy minimization (*minG*) and entropy maximization (*maxS*) models in order to study the thermochemical characterization of açai seeds. The optimization problems were formulated as nonlinear programming problems and solved using *GAMS* and *TeS* software's. The reactions studied included Pyrolysis (PR), Autothermal Reforming (ATR), Steam Reforming (SR), and Supercritical Water Gasification (SCWG). The results showed that thermochemical valorization pathways are effective for generating H<sub>2</sub> and syngas from açai seeds. Among the various processes, ATR demonstrated promising results, with good productivity of H<sub>2</sub> and syngas and nearly autothermal behavior, while SCWG achieved the high H<sub>2</sub> production, showing favorable energetic and reactional characteristics. Açai seeds has proven to be a promising alternative for energy production through thermochemical processing, offering strong potential for generation of clean and renewable energy, particularly in Brazil's açai-producing regions.

## 1. Introduction

According to 2023 data from the Brazilian Institute of Geography and Statistics (IBGE), Brazil is the world's largest producer of açai, with the highest levels of production concentrated in the North and Northeast regions. By 2021, Maranhão had ascended to third place in national açai production, harvesting over 5,000 tons of fruit, underscoring its importance in the country's açai industry. Açai production generates substantial waste, primarily in the form of seeds, which constitute about 70% of the fruit's total mass (Ribeiro et al., 2018). Given the large volume of this by-product, exploring methods to add value to açai seed waste presents a promising area for research. Thermochemical processes are vital in the search for clean, renewable energy sources and can play a key role in the thermochemical recovery of various agro-industrial by-products. These processes facilitate the conversion of residual biomass, such as açai seeds, into hydrogen—a highly efficient, low-carbon, and versatile fuel. Optimizing these processes through simulation models is essential for scaling them commercially and supporting the transition to a more sustainable energy system (Rahimi et al., 2022). Among thermochemical processes, pyrolysis (PR), steam reforming (SR), autothermal reforming (ATR), and supercritical water gasification (SCWG) are promising alternatives for the thermochemical valorization of carbon-rich biomasses like açai seeds (Zhang et al., 2025). This study seeks to apply optimization techniques to calculate combined chemical and phase equilibrium in systems relevant to the thermochemical valorization of açai seeds. The systems were analyzed using Gibbs energy minimization (at constant pressure and temperature) and entropy maximization (at constant pressure and enthalpy). Specifically, the study focuses on

the thermodynamic characterization of PR, SR, ATR, and SCWG processes. The findings of this work will contribute to a broader understanding of the thermodynamic characteristics of these processes involved in valorizing residual biomass in the açai production chain, thereby facilitating more targeted research on producing energy vectors from this underutilized raw material in Brazil.

## 2. Methodology

### 2.1 Formulation as a Gibbs energy minimization (*minG*) model

The equilibrium composition of a system with multiple components and phases, under conditions of constant pressure and temperature, can be determined by directly minimizing the Gibbs free energy of the system, taking into account the number of moles of each component in each phase. Equation 1 illustrates this approach for a system where gas, liquid, and solid phases may form (Freitas and Guirardello, 2014).

$$\min G = \sum_{i=1}^{NC} n_i^g \mu_i^g + \sum_{i=1}^{NC} n_i^l \mu_i^l + \sum_{i=1}^{NC} n_i^s \mu_i^s \quad (1)$$

where  $n_i^k$  is the number of moles of component  $i$  in phase  $k$ , and  $\mu_i^k$  is the chemical potential of component  $i$  in phase  $k$ . The restrictions for the model are found in the non-negativity of the number of moles of each component in each phase and the balance of moles obtained by the atomic balance for reactive systems (Equation 2).

$$\sum_{i=1}^{NC} a_{mi} (n_i^g + n_i^l + n_i^s) = \sum_{i=1}^{NC} a_{mi} n_i^0, \quad m = 1, \dots, NE, \quad n_i^g, n_i^l, n_i^s \geq 0 \quad (2)$$

where  $a_{mi}$  is the number of atoms of element  $i$  in component  $m$  and  $NE$  is the number of elements. The *minG* was calculated considering that the components were only on gaseous phase and there was only coke formation (represented as pure carbon,  $C_{(s)}$ ) in solid phase. These considerations were used in previous research with good results (Dos Santos et al., 2021). Equation 3 represents the Gibbs energy equation with these considerations.

$$G = \sum_{i=1}^{NC} n_i^g \left( \mu_i^g + RT(\ln P + \ln y_i + \ln \hat{\phi}_i) \right) + n_{C_{(s)}} \mu_{C_{(s)}} \quad (3)$$

Here,  $P$  represents pressure,  $T$  is temperature,  $R$  is the universal gas constant,  $y_i$  is the mole fraction of gas component  $i$ , and  $\hat{\phi}_i$  is the fugacity coefficient of component  $i$ . The *minG* model allows for the analysis of the reaction system under isothermal and isobaric conditions, meaning the operating temperature remains constant throughout the process simulation.

### 2.2 Formulation as an entropy maximization (*maxS*) model

Thermodynamic equilibrium can also be studied by maximizing the entropy of the system under conditions of constant pressure and enthalpy, as presented in Equation 4, satisfying the atom balance Eq. (2) and  $n_i^k \geq 0$ .

$$\max S = \sum_{i=1}^{NC} n_i^g S_i^g + \sum_{i=1}^{NC} n_i^l S_i^l + \sum_{i=1}^{NC} n_i^s S_i^s \quad (4)$$

where  $S_i^k$  represent the entropy of component  $i$  in phase  $k$ . The restrictions mentioned above for non-negativity of number of moles and atom balance (Equation 2) are also necessary for the *maxS* model, with the addition of conservation of enthalpy and non-negativity of absolute temperature, represented by Equation 5.

$$\sum_{i=1}^{NC} (n_i^g H_i^g + n_i^l H_i^l + n_i^s H_i^s) = \sum_{i=1}^{NC} n_i^0 H_i^0 = H^0, \quad T \geq 0 \quad (5)$$

Non-ideality in both thermodynamic models is accounted for by the fugacity coefficient, which is calculated using truncated virial equation of state, considering the second virial coefficient. The expression for the second virial coefficient is based on the correlation proposed by Pitzer (Pitzer et al., 1955), modified by Tsonopoulos (1974), as shown in Equation 6. This combination of thermodynamic formulations and equations of state has been successfully applied to reforming systems, as demonstrated in the work of Freitas and Guirardello (2014) and in Maia et al. (2024).

$$\ln \hat{\phi}_i = \left[ 2 \sum_j^m y_j B_{ij} - B \right] \cdot \frac{P}{RT} \quad (6)$$

where  $B$  is the mixture second virial coefficient and  $B_{ij}$  is the second virial coefficient for the  $ij$  pair. The *maxS* model, on the other hand, incorporates temperature variation in its thermodynamic formulation, effectively representing an adiabatic process. This model provides a more accurate behavior of the studied systems.

### 2.3 Thermodynamic analysis – computational strategy

The models used in this study perform simultaneous chemical and phase equilibrium calculations, formulated as nonlinear programming problems. For the simulations, the General Algebraic Modeling System (GAMS)<sup>®</sup> 23.9.5 software was employed, with the CONOPT3 solver. This solver utilizes the generalized reduced gradient (GRG) method, a robust algorithm for solving nonlinear programming problems, such as the *minG* and *maxS* thermodynamic models used in this work. Additionally, the free software *TeS* (Thermodynamic Equilibrium Simulation) was used for the thermodynamic characterization of açai seed reforming processes. This combination of software and solver has been successfully applied in previous studies, delivering excellent results, particularly in comparison with experimental data (Gomes et al., 2022). In the simulations, açai seeds were represented as a pseudocomponent, with their chemical composition determined through elemental analysis of seeds sourced from pulp production residue at a public market in São Luís-MA, Brazil. The resulting chemical formula was  $C_{3.90}H_{5.87}O_{2.74}N_{0.06}$ . A total of 13 compounds were considered in the simulations, including hydrogen ( $H_2$ ), methane ( $CH_4$ ), water ( $H_2O$ ), carbon monoxide (CO), carbon dioxide ( $CO_2$ ), oxygen ( $O_2$ ), nitrogen ( $N_2$ ), ammonia ( $NH_3$ ), nitric oxide (NO), nitrogen dioxide ( $NO_2$ ), methanol ( $CH_3OH$ ), ethane ( $C_2H_6$ ), and ethylene ( $C_2H_4$ ). All thermodynamic properties for these compounds were sourced from the literature (Polling et al., 2001).

ATR, PR, SR, and SCWG reactions were thermodynamically characterized for temperature ranges between 730 and 1130 K, and pressures between 1 and 20 bar for SR, PR, and ATR reactions, and between 220 and 260 bar for SCWG. The feed composition varied from 5 to 23 wt% for biomass, oxidizing agents:  $O_2$  and  $H_2O$  (in equimolar amounts) for ATR, pure  $H_2O$  for SCWG, and no oxidant for PR. The four reaction routes (PR, SR, ATR, and SCWG) were first thermodynamically evaluated in GAMS to identify those that showed the highest hydrogen gas productivity. Subsequently, the two reaction paths with the highest gas production were further detailed in *TeS* software, with over 2,000 simulations carried out for each reaction. These simulations aimed to determine the characteristic effects of each reaction and to explore the combined effects of the operational variables within each thermochemical route.

## 3. Results and discussion

The results obtained for the maximum  $H_2$  and  $CH_4$  production (determined from *minG* or *maxS* simulations) and the equilibrium temperature (starting from an initial temperature of 900 K) using GAMS software are presented in Table 1.

Table 1. Maximum  $H_2$  production, maximum  $CH_4$  production and equilibrium temperature for ATR, SR, PR and SCWG of açai seeds.

Reforming type	Maximum $H_2$ production (mol%) <sup>1</sup>	Maximum $CH_4$ production (mol%) <sup>1</sup>	Equilibrium temperature <sup>2</sup> (K)
ATR	39.2, <i>maxS</i> at 1138.7 K; 1 bar	43.1, <i>minG</i> at 730 K; 1 bar	1138.7
PR	29.2, <i>minG</i> at 950 K; 1 bar	39.8, <i>minG</i> at 730 K; 1 bar	620.3
SR	37.4, <i>minG</i> at 1000 K; 1 bar	55.4, <i>min G</i> at 730 K; 1 bar	384.5
SCWG	38.7, <i>minG</i> at 1130 K; 220 bar	48.9, <i>minG</i> at 730 K; 230 bar	892.4

<sup>1</sup>considering both simulations *maxS* and *minG*, the indication next to the number represents the reaction condition where maximum  $H_2$  production was reached, the value besides represents the temperature of the process where this production was reached. <sup>2</sup>For all thermochemical processes tested the initial temperature was fixed at 900K (intermediate value within the tested conditions).

The highest  $CH_4$  and  $H_2$  production were observed at lower pressures: 1 atm for PR, SR, and ATR, and 220 bar for SCWG. According to Table 1, SCWG and ATR reactions achieved the highest  $H_2$  molar productivity, primarily due to the high-water content in both processes, which promotes the water-gas shift reaction and enhances  $H_2$  output (Chen and Chen, 2020). Similar findings were reported by Freitas and Guirardello (2014) and Santos-Júnior et al. (2024) in studies of thermochemical conversion pathways and black liquor gasification. However, this study distinguishes itself due to the greater complexity of the açai seed biomass, which includes nitrogen and a higher C/H molar ratio, leading to more challenging operational conditions due to increased chemical reactions. The higher C/H ratio results in a larger proportion of carbonaceous compounds in the output compared to other biomass sources.

In terms of thermal behavior, the ATR process showed maximum hydrogen production at 1138.7 K, achieved using the *maxS* method (non-isothermal operation). This indicates that the ATR process for açai seeds is slightly exothermic, a trend that supports H<sub>2</sub> production in the ATR reactive system (Gomes et al., 2022). On the other hand, SR, PR, and SCWG reactions showed endothermic behavior, with the SR reaction being the most endothermic among them (Brito et al., 2023). Maximum H<sub>2</sub> production for PR, SR, and SCWG occurred during the *minG* simulations. This behavior is expected, as endothermic processes tend to be more productive under isothermal conditions, such as those simulated by the *minG* model.

Maximum CH<sub>4</sub> production occurred during *minG* simulations at lower temperatures, consistent with expectations, as higher temperatures are typically associated with CH<sub>4</sub> decomposition into H<sub>2</sub> and CO<sub>x</sub> gases. The primary nitrogen derivative across all simulations was pure N<sub>2</sub> (about 97%), with small amounts of NO and NO<sub>2</sub> (less than 10<sup>-5</sup> mol) detected in the ATR reaction, possibly due to higher oxidizing agents in the feed. NH<sub>3</sub> was also produced in small quantities (less than 10<sup>-6</sup> mol) in all simulated processes.

The highest H<sub>2</sub> production was observed in the *minG* simulations for SCWG, while the ATR reaction showed the most interesting operational behavior in *maxS* simulations. These characteristics made SCWG and ATR the most intriguing processes, prompting further analysis with *TeS* software. Figure 1 presents the results: Panel (a) shows the Spearman correlation for SCWG (*minG* model), and panel (b) shows the ATR process (*maxS* model).

The results from Figure 1 indicate that pressure had a secondary influence on SCWG for açai seeds, aligning with findings by Maia et al. (2024) for lignocellulosic biomass. Temperature significantly influenced CO and H<sub>2</sub> production, which is linked to the water-gas shift reaction. CH<sub>4</sub> exhibited a strong negative correlation with temperature, suggesting that CH<sub>4</sub> is degraded at higher temperatures, acting as an intermediate in açai seed biomass decomposition during SCWG. Ammonia formation was favored at lower temperatures, but no significant amounts were observed in the product. The direct relationship between biomass and hydrogen production was of secondary importance, indicating that the primary reaction pathway in SCWG involves intermediate compounds, like findings by Guan et al. (2012) for microalgal biomass decomposition in supercritical water.

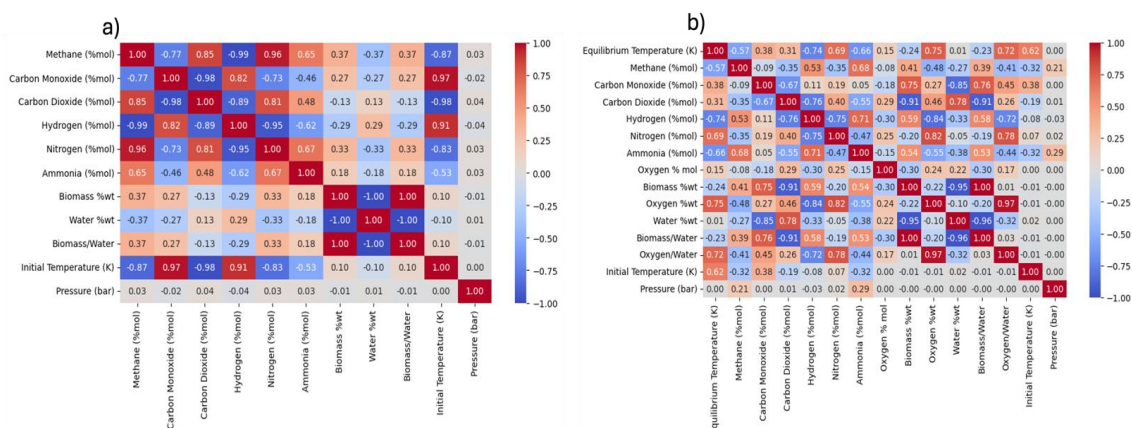


Figure 1. Spearman correlations for SCWG using *minG* model (a) and ATR using *maxS* model (b) of açai seeds.

For the ATR process, shown in Figure 1(b), pressure plays a more significant role than in the SCWG reaction discussed earlier, particularly in the production of NH<sub>3</sub> and CH<sub>4</sub>. NH<sub>3</sub>, while still a secondary product from the degradation of nitrogen in the biomass, was more favorably produced as operating pressure increased during ATR reaction. The initial operating temperature demonstrated a strong correlation with the equilibrium temperature, indicating that higher initial temperatures lead to higher equilibrium temperatures, as expected. H<sub>2</sub> production was favored at higher equilibrium temperatures, with minimal dependence on operating pressure. Unlike the SCWG process, the amount of biomass in the feed was directly proportional to the amount of H<sub>2</sub> produced in the ATR process, suggesting that different reaction pathways are followed during açai seed decomposition in SCWG and ATR. To investigate the combined effects of pressure and temperature on H<sub>2</sub> production, Figures 2 (a) and 2 (b) were constructed for the SCWG and ATR processes, respectively, with the biomass input set at 23% by weight. The SCWG process was evaluated using the *minG* model, while the ATR process was evaluated using the *maxS* model. From the results of this figure, it is evident that the ATR process produces higher total molar amounts of H<sub>2</sub> compared to the SCWG process.

The behavior of the main gaseous products ( $\text{CH}_4$ ,  $\text{CO}$ ,  $\text{CO}_2$ ,  $\text{H}_2$ , and  $\text{N}_2$ ) is shown in Figures 2 (c) and 2 (d) for the SCWG and ATR processes of açai seeds, respectively. Figure 2 (d) also includes the equilibrium temperature of the system (available only for the *maxS* model, which is non-isothermic).

Upon evaluating the results in Figures 2 (c) and 2 (d), it is clear that high molar fractions of  $\text{H}_2$  gas are produced at higher temperatures for both processes (SCWG and ATR). An interesting observation is that the ATR process operates at high temperatures, even when the initial operating temperature is lower. For example, at an initial temperature of 750 K, the equilibrium temperature (which represents the operating temperature of the system) reached 1218 K, highlighting the highly exothermic nature of the ATR process (Zhao et al., 2015). Another noteworthy trend is that the ATR process consistently produces a high molar fraction of  $\text{H}_2$ , remaining above 50% under all tested conditions.

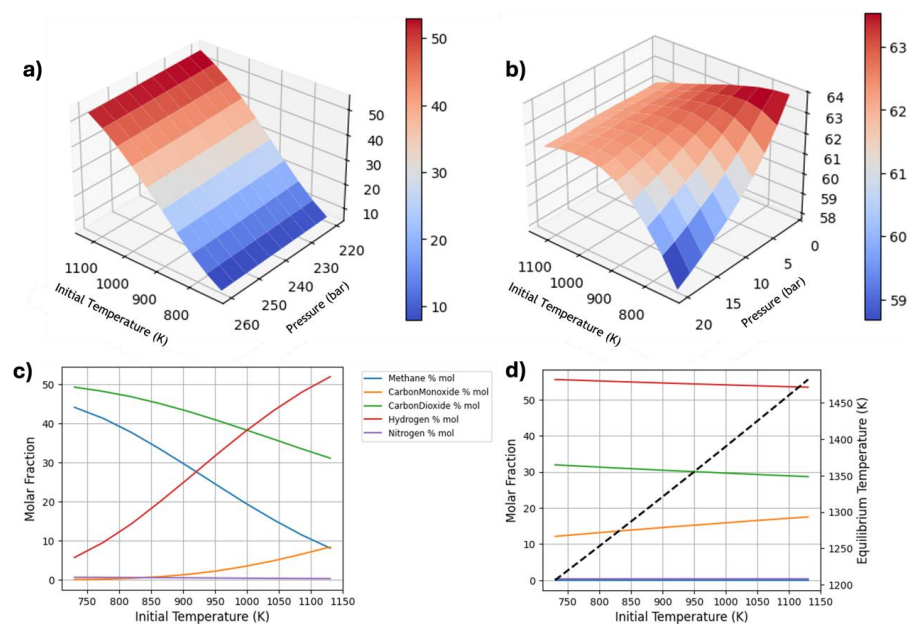


Figure 2. Response surfaces for combined effects of temperature and pressure, behavior of molar compositions and equilibrium temperature (---) resulting from the verified processes (a: SCWG for biomass equal to 23 %wt; b: ATR for biomass equal to 23 %wt; c: SCWG at 220 bar and biomass equal to 23 %wt; d: ATR at 1 bar and biomass equal to 23 %wt).

Upon further evaluation of the results presented in Figures 2(c) and 2(d), it is evident that in both cases,  $\text{H}_2$  was the primary product formed at high temperatures. In the isothermal SCWG process (Figure 2(c)), significant production of  $\text{CO}_2$  and  $\text{CH}_4$  was observed, with these being the predominant compounds in the reaction system at lower temperatures. Under the tested SCWG conditions,  $\text{CO}$  production was consistently low, never exceeding 10 mol%. The formation of products showed a strong dependence on the process temperature. Similar findings for the SCWG process are reported by Gomes et al. (2022) in their study on glycerol SCWG. In contrast, the adiabatic ATR process (Figure 2(d)) displayed less sensitivity to the initial operating temperature. This was expected, as the exothermic nature of the ATR process ensures equilibrium temperatures consistently exceeding 1100 K. Throughout the ATR process,  $\text{H}_2$  remained the dominant product, followed by  $\text{CO}_2$  and  $\text{CO}$ .  $\text{CH}_4$  was always present in low concentrations (less than 2% molar), indicating its rapid consumption in the system due to the high equilibrium temperatures achieved at ATR process.

#### 4. Conclusions

The methodologies proposed in this study have proven reliable for thermodynamic predictions in the PR, SR, ATR, and SCWG reactive systems using real biomass, represented by açai seeds in performed simulations. The approaches applied using GAMS demonstrated efficiency and speed, with computational times of less than 5 seconds for all cases analyzed. Longer computational times were observed for systems simulated using the *maxS* method compared to those using the *minG* model, due to the higher mathematical complexity of the *maxS* thermodynamic model, since in this case  $T$  is a variable too. The free software *TeS* was also found to be robust in facilitating thermodynamic analysis of various thermochemical processes, a total of 4,000

simulations were carried out in this software for the ATR and SCWG processes, with a total computational time of approximately 20 minutes. The results indicate that both the SCWG and ATR processes are promising routes for hydrogen production, achieving over 50% of the total molar fraction of H<sub>2</sub> (on a dry basis) at high operating temperatures. The analysis of operational effects and product formation suggested that distinct reaction pathways are followed in each of these thermochemical processes. Açai seeds have thus emerged as a promising feedstock for energy production through thermochemical processing, with strong potential for clean and renewable energy generation, particularly in Brazil's açai-producing regions.

### Nomenclature

$\hat{\phi}_i$ – Fugacity coefficient of component $i$ in mixture	$NC$ – Number of components
$a_{mi}$ – Number of atoms of $i$ in component $m$	$NE$ – Number of elements
$B$ – Second virial coefficient for the mixture	$n_i^0$ – Initial number of moles
$B_{ij}$ – Second virial coefficient for the $ij$ pair	$n_i^k$ – Number of moles of component $i$ in phase $k$
$g$ – Gas phase	$S_i^k$ – Entropy of component $i$ in phase $k$
$G$ – Gibbs energy	$y_i$ – Molar fraction of gas phase
$l$ – Liquid phase	$P$ – Pressure
$H^0$ – Total initial enthalpy	$R$ – Universal gas Constant
$H_i^0$ – Initial enthalpy of component $i$	$s$ – Solid phase
$H_i^k$ – Enthalpy of component $i$ in phase $k$	$T$ – Temperature
$\mu_i^k$ – Chemical potential of component $i$ in phase $k$	

### Acknowledgments

We are grateful for the financial support from the National Agency of Petroleum, Natural Gas and Biofuels (ANP) through the ANP Human Resources Training Program for the Oil and Gas Sector (PRH 54.1 - UFMA), CNPq (Conselho Nacional de Desenvolvimento Científico e Tecnológico) and FAPEMA (Fundação de Amparo a Pesquisa e ao Desenvolvimento Científico e Tecnológico do Maranhão).

### References

- Brito J., Pinto F., Ferreira A., Soria M.A., Madeira L.M., 2023, Steam reforming of biomass gasification gas for hydrogen production: From thermodynamic analysis to experimental validation, *Fuel Processing Technology*, 250, 107859.
- Chen W.H., Chen C.Y., 2020, Water gas shift reaction for hydrogen production and carbon dioxide capture: A review, *Applied Energy*, 258, 114078.
- Freitas A.C.D., Guirardello R., 2014, Comparison of several glycerol reforming methods for hydrogen and syngas production using Gibbs energy minimization, *International Journal of Hydrogen Energy*, 39, 17969-17984.
- Gomes J. G., Mitoura J., Vidotti A.D.S., Freitas A.C.D., Guirardello R., 2022, Analysis of Hydrogen Production from Glycerol Gasification using Supercritical and Subcritical Water. *Chemical Engineering Transactions*, 92, 133-139.
- Guan Q., Wei C., Savage P.E., 2012, Kinetic model for supercritical water gasification of algae, *Phys. Chem. Chem. Phys.*, 14, 3140-3147.
- IBGE, 2023, Açai Production (cultivation) Instituto Brasileiro de Geografia e Estatística < <https://www.ibge.gov.br/explica/producao-agropecuaria/acai-cultivo/br> > accessed 11.12.2024.
- Pitzer K.S., Lippmann D.Z., Curl R.F., Huggins C.M., Petersen D.E., 1955, The Volumetric and Thermodynamic Properties of Fluids. I. Theoretical Basis and Virial Coefficients *J. Am. Chem. Soc.*, 77, 3433–3440.
- Polling, B.E.; Prausnitz, J.M.; O'Connell, J.P. *Properties of Gases and Liquids*; McGraw-Hill Education: New York, NY, USA, 2001.
- Rahimi Z., Anand A., Gautam S., 2022, An overview on thermochemical conversion and potential evaluation of biofuels derived from agricultural wastes, *Energy Nexus*, 7, 100125.
- Ribeiro L.A.S., Thim G.P., Alvarez-Mendez M.O., Coutinho A.R., Moraes N.P., Rodrigues L.A., 2018, Preparation, characterization, and application of low-cost açai seed-based activated carbon for phenol adsorption. *International Journal of Environmental Research*, 12, 755–764.
- Santos-Júnior J.M., Vidotti A.D S., Freitas A.C.D., Guirardello R., 2024, Black Liquor Gasification in Supercritical Water: Thermodynamic Study for Isothermal Systems. *Chemical Engineering Transactions*, 109, 205-210.
- Tsonopoulos C., 1974, An empirical correlation of second virial coefficients, *AIChE Journal*, 20, 263–272.
- Zhang J., Gu J., Shan R., Yuan H., Chen Y., 2025, Advances in thermochemical valorization of biomass towards carbon neutrality, *Resources, Conservation and Recycling*, 212, 107905.
- Zhao H., Guo L., Zou X., 2015, Chemical-looping auto-thermal reforming of biomass using Cu-based oxygen carrier, *Applied Energy*, 157, 408-415.